Water Research 235 (2023) 119748

Contents lists available at ScienceDirect

Water Research

journal homepage: www.elsevier.com/locate/watres

Enhancing phosphorus removal of photogranules by incorporating polyphosphate accumulating organisms

Lukas M. Trebuch [a,b,*], Jasper Sohier [a], Sido Altenburg [a], Ben O. Oyserman [c,d], Mario Pronk [e,f], Marcel Janssen [b], Louise E.M. Vet [g], René H. Wijffels [b,h], Tânia V. Fernandes [a]

[a] Department of Aquatic Ecology, Netherlands Institute of Ecology (NIOO-KNAW), Droevendaalsesteeg 10, 6708 PB, Wageningen, The Netherlands
[b] Bioprocess Engineering, AlgaePARC Wageningen University, P.O. Box 16, 6700 AA, Wageningen, The Netherlands
[c] Department of Microbial Ecology, Netherlands Institute of Ecology (NIOO-KNAW), Droevendaalsesteeg 10, 6708 PB, Wageningen, The Netherlands
[d] Bioinformatics Group, Wageningen University, Wageningen, The Netherlands
[e] Department of Biotechnology, Delft University of Technology, Van der Maasweg 9, Delft, 2629 HZ, The Netherlands
[f] Royal HaskoningDHV, Laan1914 35, Amersfoort, 3800 AL, The Netherlands
[g] Department of Terrestrial Ecology, Netherlands Institute of Ecology (NIOO-KNAW), Droevendaalsesteeg 10, 6708 PB, Wageningen, The Netherlands
[h] Faculty of Biosciences and Aquaculture, Nord University, N-8049, Bodø, Norway

ARTICLE INFO

Keywords:
Wastewater
Microalgal-bacterial granules
Enhanced biological phosphorus removal (EBPR)
PhotoEBPR
Microbial ecology
Aerobic granular sludge

ABSTRACT

Photogranules are a novel wastewater treatment technology that can utilize the sun's energy to treat water with lower energy input and have great potential for nutrient recovery applications. They have been proven to efficiently remove nitrogen and carbon but show lower conversion rates for phosphorus compared to established treatment systems, such as aerobic granular sludge. In this study, we successfully introduced polyphosphate accumulating organisms (PAOs) to an established photogranular culture. We operated photobioreactors in sequencing batch mode with six cycles per day and alternating anaerobic (dark) and aerobic (light) phases. We were able to increase phosphorus removal/recovery by 6 times from 5.4 to 30 mg/L/d while maintaining similar nitrogen and carbon removal compared to photogranules without PAOs. To maintain PAOs activity, alternating anaerobic feast and aerobic famine conditions were required. In future applications, where aerobic conditions are dependent on *in-situ* oxygenation via photosynthesis, the process will rely on sunlight availability. Therefore, we investigated the feasibility of the process under diurnal cycles with a 12-h anaerobic phase during nighttime and six short cycles during the 12 h daytime. The 12-h anaerobic phase had no adverse effect on the PAOs and phototrophs. Due to the extension of one anaerobic phase to 12 h the six aerobic phases were shortened by 47% and consequently decreased the light hours per day. This resulted in a decrease of phototrophs, which reduced nitrogen removal and biomass productivity up to 30%. Finally, we discuss and suggest strategies to apply PAO-enriched photogranules at large-scale.

1. Introduction

Wastewater treatment must become more sustainable by applying technologies that recover energy and nutrients as well as removing pollutants. Recently, the commercialization of well-settling aerobic granular sludge (AGS) as NEREDA® has transformed biological wastewater treatment by increasing treatment capacity while decreasing the aerial footprint of treatment plants, and saving on energy costs (Pronk et al., 2015). Still, AGS requires a substantial amount of mechanical aeration (up to 50% of total energy costs) and emits greenhouse gasses such as CO_2 and N_2O (Brockmann et al., 2021; Pronk et al., 2015). Additionally, AGS systems are designed to convert nitrogen into N_2 rather than recovering it as biomass.

An alternative to mechanical aeration is *in-situ* oxygenation via photosynthesis. In recent years, photogranules have become a promising technology to close the CO_2 and O_2 cycles in treatment systems and thereby lower, or eliminate, the need for external aeration. Photogranules consists of phototrophs (microalgae, cyanobacteria) and other non-phototrophic microorganisms (nitrifiers, denitrifiers) that form dark green spheroid agglomerates. The principle of photogranular

* Corresponding author: Department of Aquatic Ecology, Netherlands Institute of Ecology (NIOO-KNAW), Droevendaalsesteeg 10, 6708 PB Wageningen, The Netherlands.
E-mail address: L.Trebuch@nioo.knaw.nl (L.M. Trebuch).

https://doi.org/10.1016/j.watres.2023.119748
Received 19 October 2022; Received in revised form 21 January 2023; Accepted 12 February 2023
Available online 15 February 2023
0043-1354/© 2023 The Authors. Published by Elsevier Ltd. This is an open access article under the CC BY license (http://creativecommons.org/licenses/by/4.0/).

wastewater treatment is to eliminate external O_2 supply via *in-situ* oxygenation by photosynthesis and sequester CO_2 produced internally via phototrophs. Photogranules can efficiently remove and recover carbon and nitrogen but show lower phosphorus assimilation than other established biological treatment systems (Trebuch et al., 2020).

Enhanced biological phosphorus removal (EBPR) is a widely used strategy in conventional activated sludge (CAS) or AGS systems to increase phosphorus removal. The main contributors to phosphorus removal are polyphosphate accumulating organisms (PAOs) that can accumulate vast amounts of intracellular polyphosphate (up to 0.38 mgP/mgVSS) (Chen et al., 2020). The addition of PAOs in phototrophic cultivation in suspension as photoEBPR showed improved phosphorus removal compared to phototrophic systems only (Carvalho et al., 2021, 2018; Mohamed et al., 2021; Oyserman et al., 2017). The main metabolic functions within the photoEBPR process are 1) photosynthesis, 2) polyphosphate accumulation, 3) chemoheterotrophy (COD removal), 4) nitrification and 5) denitrification. Combining all functions together in one reactor system can be difficult as competition for nutrients and inhibition (e.g., by product accumulation) can adversely affect microorganisms. Competition between phototrophs, nitrifiers and PAOs for nutrients often led to suboptimal removal rates and a decrease in PAO abundance (Carvalho et al., 2018; Mohamed et al., 2021). Additionally, nitrite-oxidizing bacteria have been shown to be sensitive to light and compete with phototrophs for CO_2 (Wang et al., 2015), while PAOs are sensitive to high nitrite and oxygen concentration (Chen et al., 2020).

Granules exhibit physical and chemical gradients (e.g., light, nutrients), which facilitate stratification and spatial heterogeneity of microbial communities (Flemming and Wingender, 2010; Trebuch, 2022). This allows for niche differentiation and the coexistence of diverse organisms even those that feed on the same substrate, or produce metabolites that negatively affect each other (Louca et al., 2018). In the context of photoEBPR, photogranules could provide niches for all organisms (phototrophs, PAOs, nitrifiers, and denitrifiers), allowing them to coexist in the same reactor while expressing high conversion rates needed for wastewater treatment. A few studies already investigated the combination of photogranules and AGS performing EBPR (Cai et al., 2019; Huang et al., 2015; Ji et al., 2020; Meng et al., 2019). However, reactor operation was often not optimized for the combination of phototrophs and PAOs, which included low and uncontrolled light input (Huang et al., 2015), light irradiation during anaerobic feeding (Huang et al., 2015; Meng et al., 2019; Cai et al., 2019), and not ideal F/M ratios with too short anaerobic feeding phases (Ji et al., 2020). This resulted in unstable operation and impaired removal rates compared to other AGS systems (de Graaff et al., 2020; de Kreuk et al., 2005; Pronk et al., 2015). For example, Huang et al., 2015, reported that the growth of microalgae on AGS deteriorated phosphorus removal by 50% compared to AGS without microalgae. Therefore, it is vital to explore strategies to effectively incorporate PAOs into photogranules, optimize operation conditions for high conversion rates and get a deeper insight into their microbial community assembly and functions.

Additionally, an important aspect of light-driven processes is its dependency on the natural diel cycle of the sun. When considering a photoEBPR system with *in-situ* oxygenation, this would lead to an extended anaerobic phase during the night. At night, phototrophs would do maintenance and respire photosynthate (e.g., carbohydrates) stored during the light period. So far, there are no reports on the (long-term) effect of an extended anaerobic phase on PAO performance and it is unknown if operating a photoEBPR system under a natural diel cycle is feasible. In this study, we integrated PAOs from AGS into an established photogranular culture and analyzed microbial community assembly and functioning. Additionally, we investigated an operation scheme that would allow the photoEBPR process to run under natural light conditions (diel cycle) with 12 h light and 12 h darkness.

2. Materials and method

2.1. Inoculation strategy and adaptation phase

Two different types of biomasses were used for inoculation: 1) photogranules (PG) and 2) aerobic granular sludge (AGS) performing enhanced biological phosphorus removal (EBPR). PG were obtained from previous research (Trebuch et al., 2020). AGS originated from the research of de Graaff et al. (2020). Both types of granules were adapted to the experimental conditions (nutrient load, salinity, pH, and temperature) for 28 days prior to the start of the actual experiment. During the experimental phase three bioreactors were operated in parallel with different inocula. 1) The first bioreactor, termed PG1, received homogenized photogranules and intact AGS in equal weight proportions (homogenization by a Miccra D9 Homogeniser; Miccra GmbH). 2) The second bioreactor, termed PG2, received both intact photogranules and AGS in equal weight proportions. 3) The third bioreactor was operated with intact AGS, which served as a benchmark for phosphorus removal via EBPR.

2.2. Bioreactor set-up and operation

Three glass bubble column bioreactors with a diameter of 10 cm, a total height of 28 cm and a working volume of 1.6 L were used (Figure S1). All three bioreactors were operated as sequencing batch reactors (SBRs) employing six cycles per day. During the co-cultivation phase of photogranules and AGS, one cycle consisted of anaerobic influent feeding (5 min) and reaction (70 min), aerobic reaction (150 min), settling (5 min), effluent removal (3 min), and nitrogen sparging (7 min) (Figure S2). The co-cultivation phase lasted for 56 days.

Mixing of the bioreactor content was achieved via gassing with nitrogen (N_2) during the anaerobic phase and with air during the aerobic phase both enriched with 5% w/w CO_2. In both phases, a gas flowrate of 0.5 L/min was maintained via mass flow controllers. Prior to feeding, the bioreactor content was sparged with N_2 gas for 7 min to remove residual O_2 and to ensure anaerobic conditions. The bioreactor temperature was kept at 20 ± 0.5 °C using external water baths and pH at 7.25 ± 0.1 by automatic addition of 1 M HCl or 1 M NaOH. Bioreactors PG1 and PG2 were illuminated during the aerobic phase with three warm white LED panels each (Figure S3). The light sources were placed at three sides of the bioreactor, with 90° between panel 1 and 2, 90° between panel 2 and 3 and 180° between panel 3 and 1. The average incident light intensity measured over the whole bioreactor surface was 170 μmol/m^2/s, with a total light input of 0.43 mol/L/day (15 h light per day).

Synthetic wastewater was prepared by mixing tap water with 10 mL/L of stock A and 10 mL/L of stock B. Stock A consisted of 42.80 g/L $CH_3COONa{\cdot}3H_2O$, 1.09 g/L KH_2PO_4 and 4.20 g/L K_2HPO_4. Stock B consisted of 6.84 g/L NH_4Cl, 7.50 g/L $MgSO_4{\cdot}7H_2O$, 3.60 g/L $CaCl_2{\cdot}2H_2O$, 3.50 g/L KCl and 100 mL/L of trace element solution prepared according to Vishniac and Santer (1957) with 2.2 g/L of $ZnSO_4{\cdot}7H_2O$ instead of 22 g/L. The concentrations of major constituents of the final synthetic wastewater were: 18 mg/L of nitrogen, 10 mg/L phosphorus and 200 mg/L of COD.

After 6 weeks (day 14 – 56) of stable C, N and P removal, one of the anaerobic phases was extended to 12 h (720 min) while maintaining an aerobic phase of 80 min. The other five cycles had equal anaerobic phases of 40 min and aerobic phases of 80 min (Figure S2). The length of the light period in PG1 and PG2 was adjusted to the aerobic phases and was therefore shorter. The overall light input was reduced from 15 h/day to 8 h/day and thereby to 0.23 mol/L/day. The extension of the anaerobic phase was done gradually over one week. It was first extended from 60 to 180 min, with subsequent extension to 350, 530 and 690 min, until finally to 720 min. The bioreactors were operated for an additional 3 weeks with a 12-h anaerobic phase.

Throughout the whole experiment a hydraulic retention time (HRT)

of 0.33 days was applied with a volume exchange ratio of 0.5 per cycle. The solids retention time (SRT) was maintained at 14 days by daily removal of 114 mL of mixed liquor. The nutrient load was 55 mg/L/d of nitrogen, 30 mg/L/d of phosphorus, and 600 mg/L/d of COD.

2.3. Analytical methods

During the experiment, liquid samples were taken from the influent and the effluent of the bioreactors to study nutrient removal. In addition, a liquid sample was taken at the end of the anaerobic phase. Once a week, one cycle (on day 4, 11, 15, 25, 30, 36, 46, and 53) or two consecutive cycles (on day 67, 73, and 79) were sampled in 5- or 10-min intervals to gain more insight in conversion kinetics. All liquid samples were filtered through 0.2 μm syringe filters (PES membrane, VWR) and analyzed for ammonium (NH_4^+-N), nitrite (NO_2^--N), nitrate (NO_3^--N), and phosphate (PO_4^{3-}-P) with a Skalar SAN^{++} autoanalyzer (Skalar Analytical B.V.) according to standard methods (APHA et al., 2012). Acetate was measured by high-performance liquid chromatography (HPLC). For more information see supplemental materials. For rapid testing of the liquid samples for PO_4^{3-}-P the PhosVer 3 kit (Hach Lange) was used. Total suspended solids (TSS), volatile suspended solids (VSS), and sludge volume index (SVI) were assessed according to standard methods (APHA et al., 2012).

2.4. Biomass characteristics and morphology

The elemental composition of homogenized freeze-dried biomass was measured. For C and N analyses, an aliquot (about 2 mg) was folded into a tin cup and analyzed in an organic elemental analyzer (Flash 2000, Interscience). Cellular P was analyzed by combusting an aliquot (about 2 mg) for 30 min at 550 °C in Pyrex glass tubes, followed by a digestion step with 10 mL persulfate (2.5%) for 30 min at 121 °C. The digested solution was measured for PO_4^{3-}-P on the Skalar SAN^{++} autoanalyzer (Skalar Analytical B.V.). Chlorophyll was extracted with ethanol (100%) from biomass samples from PG1 and PG2 according to the protocol of Cuaresma Franco et al. (2012). The full extraction protocol can be found in the supplemental materials.

Biomass samples were observed via a stereomicroscope (Leica M205C) to assess granule morphology, and the integration of photogranules and AGS. Images were taken using the Leica Application Suite v4.13. Photogranule size was determined by analyzing multiple microscopic images per sample (with a total of at least 400 particles) using ImageJ (Milferstedt et al., 2017).

2.5. Microbial community assessment and functional annotation

The microbial community of day 0, 8, 15, 31, 53, 67, and 79 was assessed using 16S and 18S rRNA gene amplicon sequencing according to Trebuch et al. (2020). The detailed DNA extraction, sequencing, and processing of sequencing reads can be found in the supplemental materials. The raw 16S and 18S rRNA gene sequence data is available in the EBI database under project number PRJEB54716. The 16S dataset was annotated with functions using the tool FAPROTAX (Louca et al., 2016). The default database of FAPROTAX was extended with taxa functionally annotated within the MiDAS database (version 4.8.1) (Nierychlo et al., 2020). It is important to note that several functions can be annotated to one single taxon and consequently sum of the functional distribution can exceed 100%.

3. Results

3.1. Assembly of PG+: photogranules enriched with polyphosphate accumulating organisms

In this study we successfully combined photogranules (PG) with aerobic granular sludge (AGS) enriched with polyphosphate accumulating organisms (PAOs) to form PG enriched with PAOs, named PG+. PG+ were operated as a phototrophic enhanced biological phosphorus removal (photoEBPR) system. To investigate the assembly of PG+, two different inoculation strategies were tested: 1) PG were mechanically homogenized and co-cultivated with intact AGS (referred to as PG1). 2) Both PG and AGS were kept intact and co-cultivated (referred to as PG2). The co-cultivation phase lasted for 56 days and the assembly of the PG+ was followed via microscopic observations (Fig. 1).

The first PG+ appeared in both PG1 and PG2 after one week of cultivation. They arose among intact native PG (in PG2) and AGS. Within 2–3 weeks of operation, the bioreactors were completely dominated by PG+. Most PG+ were in the range of 0.8 − 1.4 mm in diameter with a maximum of 1.8 mm. The morphology of PG+ was characterized by an interwoven network of cyanobacteria with cauliflower shaped aggregates of AGS in between (white areas on surface) (Fig. 1). While the PG+ morphology of PG1 and PG2 was similar, two modes of assembly could be identified depending on the size and morphology of the initial PG and AGS. In the first mode of assembly, especially in the PG1 treatment, AGS were colonized by the homogenized microbial community of PG and were gradually overgrown by phototrophic organisms (Fig. 1, upper path). Over time, the phototrophs covered the whole surface and formed a thick mat with PAO colonies protruding the surface. This eventually resulted in the typical PG+ morphology. The second mode of assembly was PG being colonized by small to medium sized AGS (Fig. 1, lower path). Over time, the AGS were incorporated into the PG and finally formed mature PG+ similar to the ones obtained via the first mode of assembly.

3.2. Bioreactor performance of PG+ and AGS

During the co-cultivation phase, all three bioreactors (PG1, PG2, AGS) were operated with 6 cycles per day with 70 min of anaerobic (dark) and 150 min of aerobic (light) phase. Despite the different inoculation strategies of PG1 and PG2, their performance during steady state was similar, reaching full removal of nitrogen, phosphorus, and COD already after one week of operation (53 ± 1 mgN/L/d, 29.9 ± 0.5 mgP/L/d and 600 mgCOD/L/d) (Figure S4). Phosphorus release and reuptake dynamics were similar in all three bioreactors with maximum release concentrations of about 60 mgP/L (Fig. 2A-C), while AGS showed the highest specific phosphorus release with 25 mgP/gVSS compared to 10 and 12 mgP/gVSS for PG1 and PG2. The acetate was quickly consumed in all three bioreactors at similar rates. Ammonium concentrations were relatively stable during the anaerobic phase and ammonium was primarily consumed during the aerobic phase. All three bioreactors showed excellent settling properties with average SVI values from day 10 to day 56 of 49 ± 3 mL/g (PG1), 52 ± 3 mL/g (PG2) and 42 ± 3 mL/g (AGS) (Figure S5), and average effluent concentrations of 24 ± 15 mgTSS/L (PG1), 67 ± 72 mgTSS/L (PG2) and 15 ± 3 mgTSS/L (AGS) (Figure S6).

Both PG1 and PG2 showed full nitrogen removal, while AGS achieved 50–60% removal. The phototrophs in PG1 and PG2 could make use of light energy and consequently had double the biomass productivity, which resulted in 2–3x higher biomass concentration, 5.9 ± 0.5 gVSS/L in PG1 and 5.2 ± 0.5 gVSS/L in PG2, compared to 2.2 ± 0.2 gVSS/L in AGS (Figure S6). Due to the difference in biomass concentration despite similar bioreactor performance, the specific removal rates for COD and P observed for PG1 and PG2 were 2–3x lower compared to AGS (Figure S7–10). The phosphorus content in the biomass of AGS was more than double (12.3%w/w) compared to in PG1 and PG2 (4.6%w/w) (Fig. 2D). Overall PG+ showed 4–5x higher phosphorus recovery potential than native PG, which exhibited about 1%w/w of phosphorus in their biomass.

AGS showed nitrification activity of maximum 5 mgN/L/d (3.3 mgN/gVSS/d), which helped with ammonium removal but not with overall nitrogen removal. Denitrification may have occurred but was not investigated in this study. The dissolved oxygen (DO) concentration

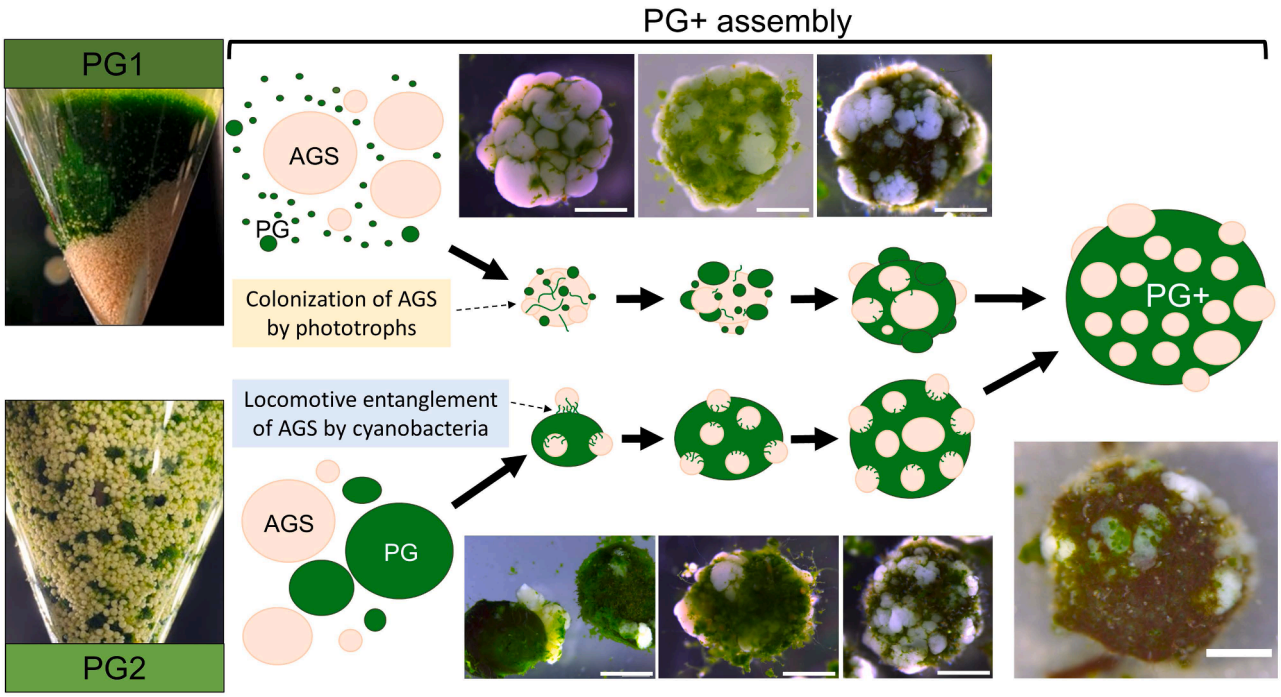

Fig. 1. Schematic representation of PG+ assembly. Photogranules (PG) and aerobic granular sludge (AGS) were co-cultivated for 56 days and the incorporation of both types of granules into the hybrid granule PG+ were followed via microscopy. The white bar in the microscopic images is a scalebar of 500 μm. Two different starting inoculants were used: PG1) Homogenized PG and intact AGS. PG2) Intact PG and intact AGS. Two main modes of PG+ assembly were postulated: 1) AGS are gradually overgrown by the microbial community of homogenized photogranules or small PG attaching to the surface of the AGS (upper path). 2) Both PG and AGS are intact, and the surface of the PG are gradually colonized with small sized AGS (lower path). (For interpretation of the references to color in this figure legend, the reader is referred to the web version of this article.)

during the aerobic (light) phase increased for both PG1 and PG2 in a similar fashion and reached a maximum concentration of about 12 mg/L at the end of the phase. For AGS, the DO increased over the course of the aerobic phase and peaked at around 6 mg/L. This was a clear difference due to the *in-situ* oxygenation via phototrophs in PG1 and PG2. In all three bioreactors the DO rose further once all phosphorus was taken up, suggesting reduced respiration by PAOs and other heterotrophs.

3.3. The effect of a 12-h anaerobic phase on PG+ and AGS systems

To test the PG+ performance under natural light conditions, we extended one of the anaerobic cycles to 12 h, thus simulating the night in a diurnal cycle. The overall light input decreased by 47% because the inclusion of the 12-h anaerobic (dark) phase required shortening of the aerobic (light) phases to preserve the feast-famine regime throughout the rest of the cycle. The reduction of the light input resulted in an equivalent decrease in phototrophic biomass productivity and a decrease in the biomass concentration over time (Fig. 3D and S3). Thereby the overall nitrogen assimilation also decreased and overall nitrogen removal in PG1 and PG2 was reduced by 12–16% (Fig. 3F). Similar to AGS, PG1 established an active nitrifying community which contributed to full ammoniacal nitrogen removal. The nitrifying activity was low and comparable to the one of AGS, with 5 mg/L/d turned over. PG2 had only marginable conversion of ammonium into nitrite or nitrate and thereby did not show full ammoniacal nitrogen removal. Generally, AGS was not affected by the change in operation conditions and maintained similar biomass productivity, biomass concentration and specific removal rates to that seen during the co-cultivation phase (Fig. 3, Figure S7–10).

Phosphorus release and reuptake dynamics were almost identical for all three bioreactors and comparable to the co-cultivation phase. Interestingly, the release during the 12-h anaerobic phase (max. 62 mg/L of phosphorus) was higher than in the subsequent 40 min anaerobic phases (max. 54 mg/L of phosphorus) (Fig. 3A-C). Still the total phosphorus removal was complete in all three bioreactors. The specific phosphorus release of AGS stayed almost equal releasing 24 mgP/gVSS compared to 25 mgP/gVSS during the co-cultivation phase. The specific phosphorus release rate for PG1 and PG2 was lower, releasing 7 and 8 mgP/gVSS compared to 10 and 12 mgP/gVSS during the co-cultivation phase (Fig. 2E and Fig. 3E). The SVI of PG1 and PG2 increased slightly to 52 ± 5 mL/g and 55 ± 4 mL/g, while the SVI of AGS decreased to 36 ± 1 mL/g (Figure S5). Average biomass concentrations in the effluent of all three bioreactors were similar at about 20 mg/L (Figure S6).

3.4. Microbial community analysis and functional annotation

During the co-cultivation phase and the extension of the anaerobic phase to 12 h, chlorophyll-a and chlorophyll-b were measured as an indication of the fraction of phototrophic biomass (Fig. 4). PG1 and PG2 had different starting chlorophyll concentrations (PG1 = 23 mg/gVSS and PG2 = 18 mg/gVSS) but showed similar values at the end of the co-cultivation phase to about 28 mg/gVSS. The extension of one anaerobic phase to 12 h had a strong effect on the phototrophic community. The light input was reduced by 47% and that led to a decrease of the phototrophic biomass fraction of 40–50% during the last 3 weeks of operation.

The microbial community of PG, PG1, PG2 and AGS was analyzed both with 16S and 18S rRNA gene amplicon sequencing. When looking from the inoculum to the end of the experiment the prokaryotic community converged for PG1 and PG2 in the last three sampling points, showing the strong selective effect of operating the bioreactors as photoEBPR (Fig. 5). The photogranular inoculum consisted of a diverse prokaryotic community of several cyanobacteria (e.g., *Cephalothrix komarekiana, Alkalinema pantanalense, Leptolyngbya boryanum, Pseudanabaena biceps*) and chemoheterotrophic organisms (e.g., *Thauera* sp., *Zoogloea* sp., *Prosthecobacter* sp. and *Shinella* sp.) (Figure S14). At the end

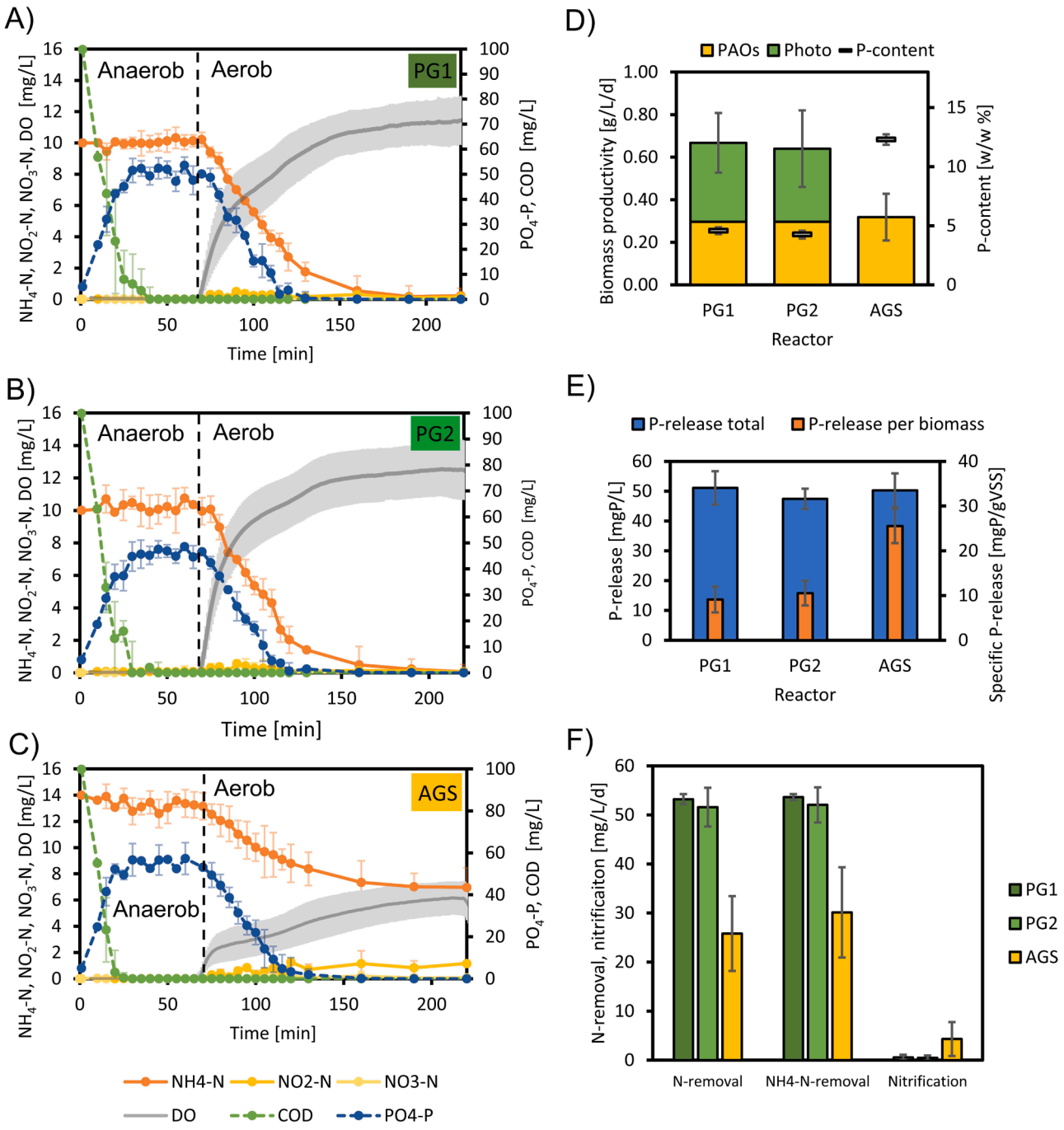

Fig. 2. Bioreactor performance of PG1, PG2 and AGS during the co-cultivation phase from day 0 to day 56. In panel A, B and C the dynamics of ammonium (NH_4-N), nitrite (NO_2-N), nitrate (NO_3-N), phosphate (PO_4-P), COD and dissolved oxygen (DO) during one sequencing batch cycle are shown for PG1 (A), PG2 (B) and AGS (C). One sequencing batch cycle consisted of a 70 min anaerobic phase and a 150 min aerobic phase. The values represented are averages of 8 cycles (day 4, 11, 15, 25, 30, 36, 46, and 53). D) Average biomass productivity of PG1, PG2 and AGS with corresponding elemental phosphorus content of the biomass. The biomass productivity of PG1 and PG2 is divided into phototrophic and PAO biomass productivity based on theoretical calculations. E) Total phosphorus release and specific phosphorus release shown for PG1, PG2 and AGS. F) Average total inorganic nitrogen (TIN), ammonium (NH_4-N) removal and nitrification rates of PG1, PG2 and AGS. The error bars in all figures represent the standard deviation of measurements. (For interpretation of the references to color in this figure legend, the reader is referred to the web version of this article.)

of the co-cultivation phase (day 53) and 12-h anaerobic phase, the community was simplified (day 67 and 79) (Figure S15). *Alkalinema pantanalense* became the dominant filamentous cyanobacteria and most abundant prokaryotic organism in PG1 and PG2, while the abundance of chemoheterotrophs *Thauera* sp. and *Zoogloea* sp. were below 1%. *Candidatus* Accumulibacter sp. *and Tetrasphaera* sp. became the dominant PAOs making up about 52% in AGS and 7–15% in PG1 and PG2 after enrichment. Other PAOs such as *Dechloromonas* sp. and *Halobacter* sp. were also present in all three bioreactors but in low abundance (1–3%). Nitrifiers (*Candidatus* nitrotoga and *Nitrosomonas* sp.) were abundant in small amounts (below 1%) in all three bioreactors, with AGS and PG1 as the only two bioreactors showing nitrifying activity.

The eukaryotic community in PG1 and PG2 was characterized by green algae (*Botryosphaerella* sp., *Chlorella* sp., *Chlorococcum* sp. and *Desmodesmus* sp.) (Fig. 5B, Figure S14). Similar to the prokaryotic community the eukaryotic algal community started off more diverse and

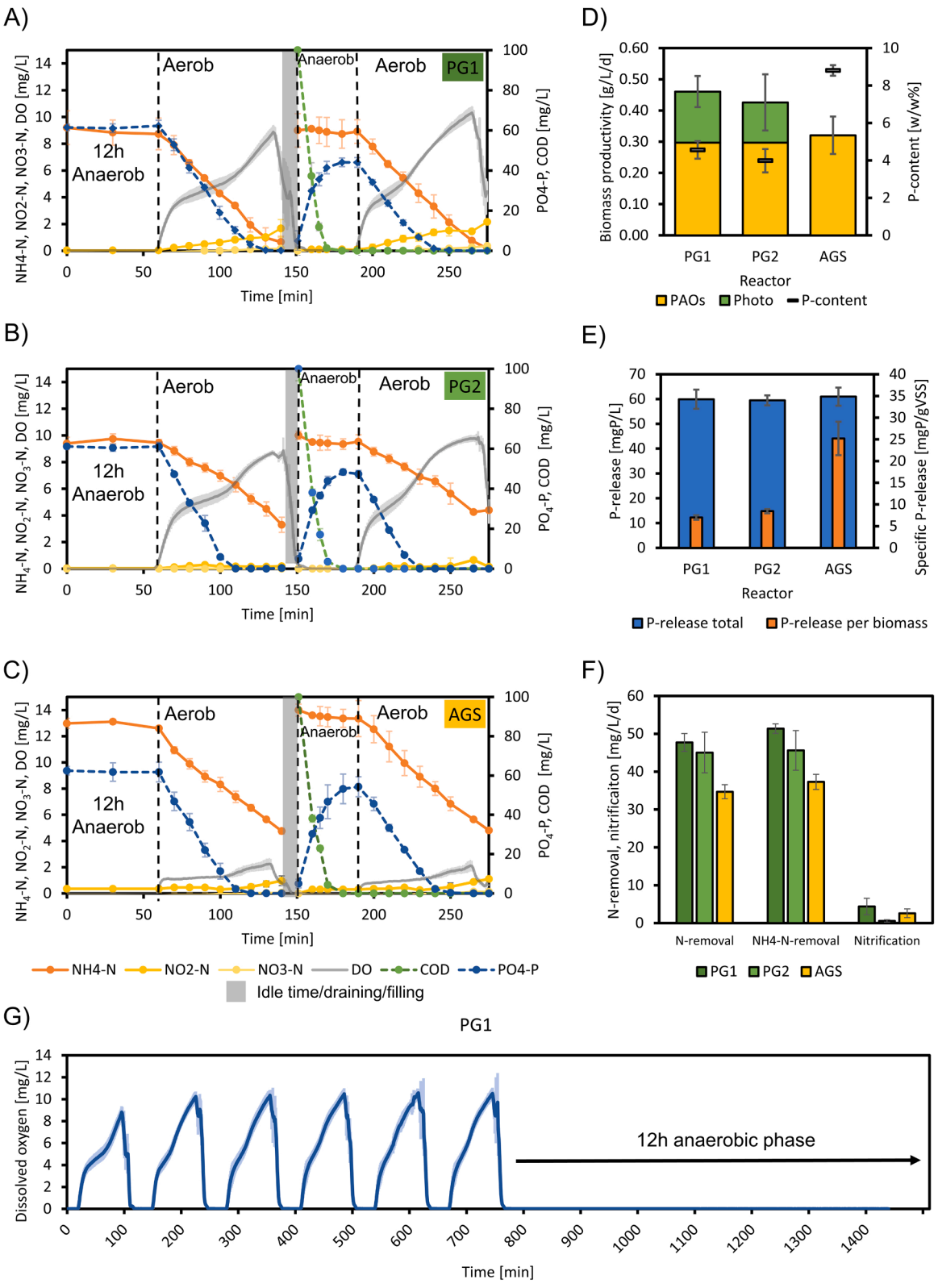

Fig. 3. Bioreactor performance of PG1, PG2 and AGS during the 12-h anaerobic phase from day 56 to day 80. The graphs shown are from the last 60 min of the 12-h anaerobic phase and the subsequent cycle consisting of a 40 min anaerobic phase and an 80 min aerobic phase. In panel A, B and C the dynamics of ammonium (NH_4-N), nitrite (NO_2-N), nitrate (NO_3-N), phosphate (PO_4-P), COD and dissolved oxygen (DO) during one sequencing batch cycle are shown for PG1 (A), PG2 (B) and AGS (C). The gray area between aerobic and anaerobic phase indicates draining and filling of the bioreactor. The values represented are averages of 3 cycles day 67, 73, and 79). D) Average biomass productivity of PG1, PG2 and AGS with corresponding elemental phosphorus content of the biomass. The biomass productivity of PG1 and PG2 is divided into phototrophic and PAO biomass productivity based on theoretical calculations. E) Total phosphorus release and phosphorus release per amount of biomass shown for PG1, PG2 and AGS. F) Average total inorganic nitrogen (TIN), ammonium (NH_4-N) removal and nitrification rates of PG1, PG2 and AGS. The error bars in all figures represent the standard deviation of measurements. G) Average DO concentration over 24 h from day 56 to day 80. (For interpretation of the references to color in this figure legend, the reader is referred to the web version of this article.)

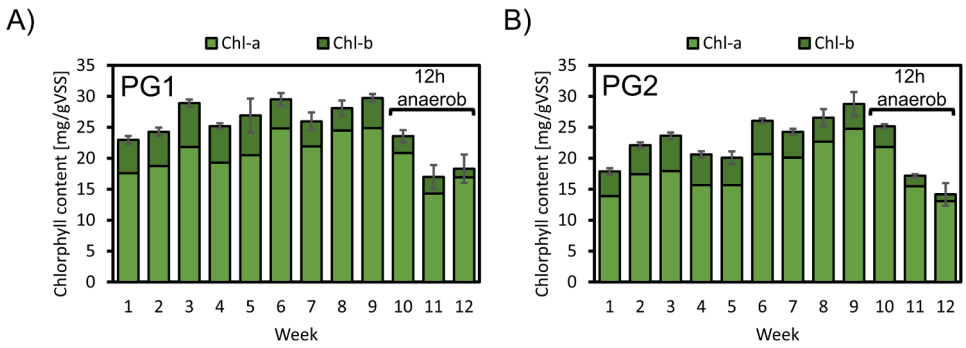

Fig. 4. Chlorophyll-a and chlorophyll-b content per amount of biomass (VSS) for PG1 (A) and PG2 (B). The average chlorophyll-a and chlorophyll-b content is displayed per week of operation. In the last 3 weeks the bioreactor operation was changed to a 12-h anaerobic (dark) phase. (For interpretation of the references to color in this figure legend, the reader is referred to the web version of this article.)

converged to a simplified community, with *Chlorella* sp. and *Desmodesmus* sp. as dominant green algae at the end of the co-cultivation phase (Fig. 5D). Next to eukaryotic algae, other organisms such as amoeba, rotifers and fungi were detected in PG1 and PG2 (2–11%). The eukaryotic community of AGS was characterized by only amoeba, rotifers and fungi, and an absence of eukaryotic algae.

The functional annotation of the 16S dataset revealed different distributions of functions for AGS, PG, PG+ and PG+(12 h). AGS was dominated by PAOs (54%), nitrification (1%) and denitrification (55%) while PG was characterized by photosynthesis (48%), chemoheterotrophy (52%), nitrification (0.2%) and denitrification (7%) (Fig. 6 and Table 1). The hybrid granule PG+ showed photosynthesis (58%), PAO (10%), chemoheterotrophy (36%), nitrification (1%) and denitrification (10%). When extending one anaerobic phase to 12 h in PG+(12 h) photosynthesis was reduced by 4% and glycogen accumulating organisms (GAO) activity started to appear with 21% of organisms performing glycogen accumulation.

4. Discussion

4.1. PG+ assembly and granule morphology

Biofilm structures such as granules are largely determined by substrate concentration gradients at the biofilm-liquid interface, the detachment forces working on the biofilm (hydrodynamic shear), the biomass yield and extracellular polymeric substance (EPS) production (Loosdrecht et al., 1997). The key for AGS formation was the introduction of an anaerobic feeding phase followed by an aerobic reaction phase. In this operation scheme, PAOs and GAOs incorporate COD anaerobically as storage polymers (PHA) and grow on these aerobically. That yields a lower aerobic growth rate compared to heterotrophic bacteria, but results in dense and sturdy biofilms (de Kreuk and van Loosdrecht, 2004). The granulation further relies to some extent on hydrodynamic conditions in sequencing batch reactors or plug flow reactors, where shear force can determine granule morphology (Nancharaiah and Kiran Kumar Reddy, 2018).

Photogranules formation was proven to work differently and is not necessarily dependent on specific operation schemes. Motile filamentous cyanobacteria govern photogranulation by the generation of extracellular polymeric substances (EPS) and locomotive entanglement (Milferstedt et al., 2017; Trebuch et al., 2020). This has been shown to work both in hydrodynamic conditions in sequencing batch reactors and also in static incubations, confirming that external drivers such as hydrodynamic shear, washout, and fluctuating chemical conditions are not necessary for photogranulation (Gikonyo et al., 2021; Milferstedt et al., 2017).

PG+ assembled rapidly from a diverse and species rich inoculum of PG and AGS and showed full treatment capacity 1–2 weeks after inoculation. The interplay of filamentous cyanobacteria (i.e., *Alkalinema pantanalense*) forming a complex network and AGS (i.e., PAOs) forming cauliflower shaped agglomerates were crucial for PG+ assembly. On one hand, the filamentous cyanobacteria formed mat-like structures in photogranules that served as a harbor for other organisms to embed themselves in (Milferstedt et al., 2017). On the other hand, the motility of filamentous cyanobacteria could actively capture and incorporate microbial communities such as AGS into the photogranules structure. This locomotive entanglement of particles (e.g., sand grains) by cyanobacteria was previously observed in natural occurring photogranules, such as cryoconites or microbialites (Brehm et al., 2003; Takeuchi et al., 2001). Further, the cauliflower-shaped agglomerates of AGS provided the phototrophic organisms a rugged surface to attach to. The early attachment of the PG microbial community on AGS occurred especially in cracks and crevices. These assembly mechanisms manifested in the two identified PG+ assembly modes described in

Fig. 1. Smaller homogenized PGs colonized the surface of larger AGS (Fig. 1, upper path) or AGS were incorporated by locomotive entanglement of intact PG (Fig. 1, lower path). The particle size ratio of PG (intact or homogenized) to AGS might have been relevant in determining which assembly pathway predominates.

4.2. PG+ functions and functional redundancy

The desired functional groups in PG+ are: 1) oxygenic photosynthesis, 2) polyphosphate accumulation, 3) chemoheterotrophy (COD removal), with 4) nitrification and 5) denitrification as optional functions to enhance overall nitrogen removal. Representatives of these functions were presented above (Figs. 5 and 6). In complex and diverse microbial communities, each function or metabolism can often be performed by multiple taxonomically distinct organisms (Louca et al., 2016). Due to the specific and selective operation conditions (feast-famine) the microbial community was simplified (Figure S14 and S15) but still had at least 5 taxa per function that were capable of the same metabolism. This established a functional redundancy that is important for the resilience of the microbial community (and functions) to biotic and abiotic influences (environmental perturbations).

Although the microbial community composition in the beginning of the co-cultivation phase was still changing (Fig. 5), the bioreactor performance was stable (Figure S4–10) confirming functional redundancy in the PG+ system. Functional stability during taxonomic fluctuations is a commonly observed phenomenon in natural ecosystems and biological wastewater treatment systems (Wang et al., 2011). Another example for functional redundancy is the taxonomic change in the functional group of chemoheterotrophs and denitrifiers during the assembly from PG to PG+. *Thauera* and *Zoogloea* are prominent representatives of these functional groups in photogranules (Trebuch et al., 2020). In PG+ they were outcompeted by PAOs (and GAOs) that consumed all acetate during the anaerobic phase leaving no organic carbon substrate in the bulk liquid for *Thauera, Zoogloea* to grow during the aerobic phase.

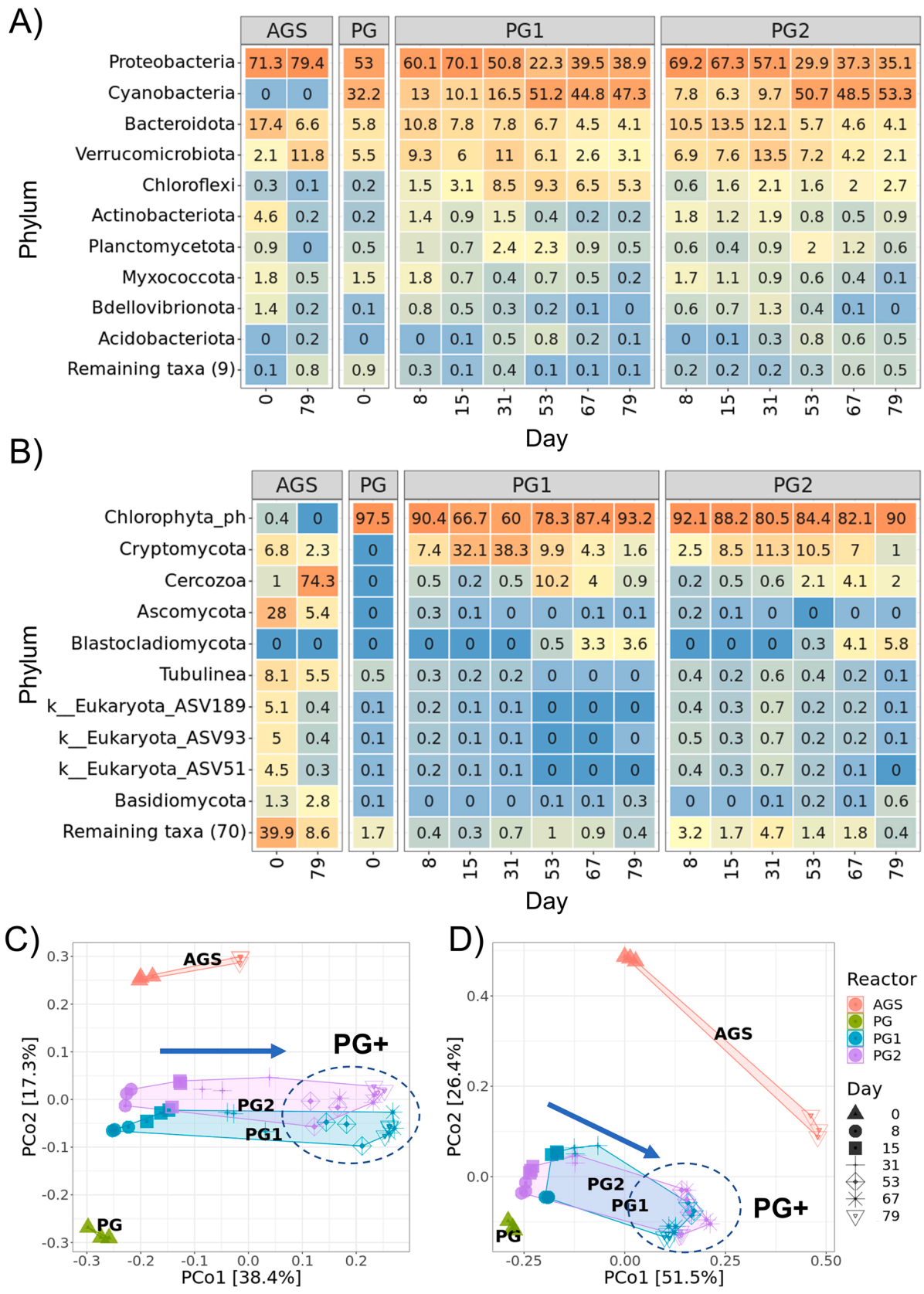

Fig. 5. Microbial community composition of PG, PG1, PG2 and AGS assessed with 16S rRNA gene (A) and 18S rRNA gene (B) amplicon sequencing displayed from the inoculum (day 0), co-cultivation phase (day 8–53) and 12-h anaerobic phase (day 67 and 79). The abundance of the top 10 phyla is presented as the average of biological replicates. The remaining phyla are summarized as "remaining taxa". Most phyla from the 18S dataset were unclassified and ASVs are presented instead. A principal coordinate analysis (PCoA) using weighted UniFrac distance of the raw data is shown (without averaging biological replicates) for 16S (C) and 18S (D). (For interpretation of the references to color in this figure legend, the reader is referred to the web version of this article.)

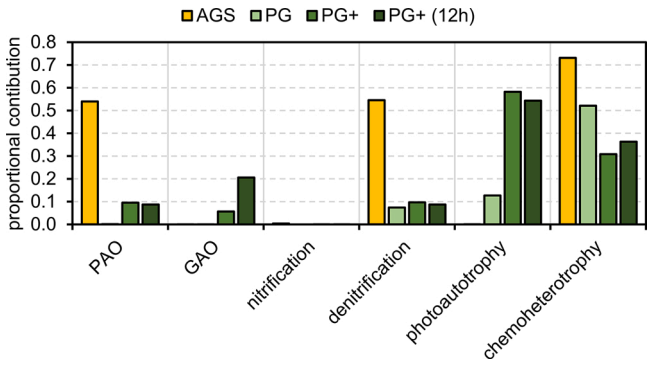

Fig. 6. Bar plot of functional attribution of 16S rRNA gene sequences found in AGS, PG, PG+ and PG+ with a 12-h anaerobic phase (PG+(12 h)). The functions were assigned using FAPROTAX. The default database of FAPROTAX was extended by functional annotations provided by MiDAS. Functions are assigned according to taxonomy, where one taxon can have multiple functions. Therefore, the functional annotation can exceed 1.0 (or 100%). In Table 1 the functions considered, the number of attributed taxa and the most prominent representatives are listed. (For interpretation of the references to color in this figure legend, the reader is referred to the web version of this article.)

Table 1
The functions assign by FAPROTAX, the number of attributed taxa and the most prominent representatives are listed.

Function	Nr. Taxa (Nr. Genus)	Representatives
PAO	46 (6)	*Tetrasphaera*, Candidatus *Accumulibacter, Dechloromonas*
GAO	39 (3)	Candidatus *Competibacter,* Candidatus *Contendobacter*
Nitrification	5 (3)	Candidatus *Nitrotoga, Nitrosomonas, Nitrosomonadaceae oc32*
Denitrification	62 (7)	Candidatus *Accumulibacter, Thauera, Zoogloea*
Phototrophy	56 (7)	*Cephalothrix, Alkalinema, Leptolyngbya, Pseudanabaena*
Chemoheterotrophy	248 (68)	Candidatus *Accumulibacter*, *Thauera, Zoogloea*

Abbreviation: PAO: polyphosphate accumulating organism. GAO: glycogen accumulating organism.

Besides the very specific polyphosphate metabolism of PAOs, they can also perform chemoheterotrophy and denitrification that can replace the functions of *Thauera* and *Zoogloea*.

The high activity of polyphosphate cycling in AGS and PG+ suggests that the actual abundance of PAOs might be higher than determined by 16S rRNA gene amplicon sequencing (Fig. 5 and S14). The relative abundance might differ from actual biomass fractions due to DNA extraction biases, primer biases, and variation in cell size and 16S/18S rRNA gene copy number between species (Albertsen et al., 2015). This issue of underrepresentation was especially evident for PAOs when investigating microbial communities in conventional wastewater treatment systems (Stokholm-Bjerregaard et al., 2017). Other techniques, such as staining PAOs with fluorescence *in-situ* hybridization (FISH) probes (Weissbrodt et al., 2013) or a recently suggested *de-novo* proteomics approach (Kleikamp et al., 2021) might show a higher enrichment of PAOs in AGS and PG+.

4.3. PG+ wastewater treatment performance

Compared to previous photogranules and non-granular photoEBPR systems (Abouhend et al., 2018; Ji et al., 2020; Mohamed et al., 2021), COD and nitrogen removal were improved by 2–3x in PG+, expect for PG where similar N removal was found (Trebuch et al., 2020). P removal was enhanced by 3–6x due to integration of PAOs into the PG+. The overall removal capacity and removal kinetics for phosphorus and COD of PG+ were consistent with other lab-scale operated AGS systems while showing higher rates of nitrogen assimilation into biomass (de Graaff et al., 2020; de Kreuk et al., 2005). The introduction of photosynthesis led to a two-fold increase in biomass productivity and nitrogen removal in PG+, while maintaining the same COD removal and phosphorus dynamics as AGS. Generating metabolic energy from light also simultaneously produced oxygen for heterotrophic activities. *In-situ* oxygenation via photosynthesis increases the association of phototrophs and heterotrophs via the exchange of O_2 and CO_2. Further, it can reduce or even remove the need for mechanical aeration, which potentially could save up to 50% of the total energy costs currently needed in conventional wastewater treatment (Brockmann et al., 2021).

PG+ achieved full removal of COD, N, and P before the end of the cycles, indicating that a larger removal capacity is surely attainable. COD was already fully consumed after 20 min into the anaerobic feeding phase (total 70 min) (Fig. 2 and 3), while P reuptake was completed 60 min into the aerobic phase (total of 150 min) and N was completely removed after 100 min. The early N and P depletion during the aerobic phase possibly hindered phototrophs from functioning at maximum capacity and nitrifiers from fully establishing. Further, PAOs would be able to cope with higher COD and P loads, as demonstrated in previous studies (de Graaff et al., 2020; de Kreuk et al., 2005). This suggests that the nutrient load in general can be increased. Increasing COD and P load would lead to an increased enrichment of PAOs and ease competition for P. Additionally, an increased N load could facilitate simultaneous nitrification and denitrification, which can occur in the aerobic and anoxic zones of granules with sizes of >1.5 mm (de Kreuk et al., 2005; Pronk et al., 2015).

Combining phototrophs and PAOs in photoEBPR systems can also have adverse effects. Cai et al. (2019) observed an increase in nitrogen removal due to the growth of phototrophs, but phosphorus removal by PAOs appeared to be hindered and consequently lowered. A similar observation was reported previously by Huang et al. (2015). They concluded that light and phototrophs inhibited nitrite oxidizing bacteria (NOB) and nitrite accumulation in the bioreactor led to inhibition of PAOs, which are sensitive to elevated nitrite concentrations (Pijuan et al., 2010). Nitrification is frequently observed in photogranules (Abouhend et al., 2018; Tiron et al., 2015; Trebuch et al., 2020), but did not fully establish in PG+. This can be attributed to competition for CO_2 and ammonium (Risgaard-Petersen et al., 2004), which was rapidly consumed in the PG+ systems. However, at elevated ammonium concentrations nitrite accumulation could become an issue and should be investigated.

4.4. How to fit the PG+ process into a natural diurnal cycle

Light is a primary energy input for PG+ and will majorly constrain the treatment capacity of the system. By using natural light, instead of artificial light, we maximize the utilization of the sun's energy with minimum energy losses, making it more sustainable and economically feasible (Blanken et al., 2013). High sunlight input throughput the year therefore will be crucial for the efficiency of the PG+ process. This favorable condition can be found predominantly in lower latitude countries with higher light input year-round (Slegers et al., 2013).

In a light-driven wastewater treatment system operated under natural light conditions all daylight should be used as efficiently as possible. When operating a PG+ system as sequencing batch reactor, the culture must be temporarily shaded in the daytime during the anaerobic phases and consequently valuable light energy remains unused. This was seen in the decrease of phototrophs and nitrogen removal in PG+ when accommodating 6 short cycles within the 12 h daytime and having a 12-h anaerobic phase (Fig. 2-4). Instead of operating in a time-based manner in one reactor vessel (sequencing batch reactor with defined phases in-time) it could be more advantageous to design the process in-space.

Recently, the AGS process was performed continuously as plug-flow, with defined reactor compartments for each phase (Li et al., 2021; Sun et al., 2019). From these studies valuable insights can be gained about how to operate a PG+ system at large scale. A plug-flow system would allow the treatment process to run continuously and have an aerobic compartment illuminated throughout the entire day, utilizing all light energy. It is important that the continuous system is designed and operated in a way that photogranules formation and functioning at high rates are still facilitated.

Although a 12-h anaerobic phase had no negative effect on phosphorus cycling of PAOs, there was a proliferation of GAOs towards the end of the 3 weeks experimental phase. PAOs and GAOs have a similar metabolism and compete anaerobically for the organic carbon source (acetate in this study). While GAO can proliferate in the same feast-famine conditions as PAOs, they do not have the benefit of using polyphosphate as an intermediate energy storage, and can only use glycogen (Chen et al., 2020). This results in strongly decreased phosphorus removal in GAO dominated systems (Lopez-Vazquez et al., 2009). While phosphorus removal was not affected in the 3 weeks of operating at a 12-h anaerobic phase, the proliferation of GAOs in photogranular systems should be investigated in future studies.

4.5. Advantages and shortcomings of a PG+ wastewater treatment system

The advantage of including phototrophic, chemoautotrophic (nitrifiers) and heterotrophic (PAOs, denitrifiers) processes in one system is that overall biomass productivity, and thereby biomass assimilation of nutrients, was increased. Currently, high biomass productivity is not desired in conventional treatment systems since it can have a significant impact on the operational costs, due to sludge disposal (Cieślik et al., 2015). However, using the produced biomass as a resource could transform wastewater treatment systems into valuable resource recovery facilities, where besides the major elements (C, N, P) microelements (e.g., Fe, Mo, Zn, Cu) are also reclaimed and transformed (Kehrein et al., 2020; Suleiman et al., 2020). The whole biomass could be used either as fertilizer (C, N, P, and microelements) or fractionated for extracellular polymeric substances (EPS) or polyhydroxyalkanoates (PHA) for biopolymer production (Kehrein et al., 2020). Including phototrophs into the treatment system can potentially extend the product range of the biomass by e.g., photopigments, lipids, proteins, and antioxidants (Borowitzka, 2013).

PG+ rapidly assembled from PG and AGS and showed resilience to a 12h-anaerobic phase. This suggests that the PG+ process can be quickly established and is suitable to be operate under a natural diel cycle. A hurdle for PG+ application, as for all light driven processes (e.g., phototrophic microalgal production), is the design of a full-scale system. Photobioreactors need a high surface to volume ratio to harness light. Common designs are closed tubular systems or shallow (20–40 cm deep) open raceway ponds. Consequently, light-driven wastewater treatment will have larger areal footprints compared to conventional wastewater treatment techniques, such as CAS or AGS. Nevertheless, this disadvantage of the PG+ system will be outweighed by its advantages: using the sun's energy for lowering or eradicating mechanical aeration and producing valuable biomass for nutrient recovery and other raw materials (EPS, bulk chemicals).

Transitioning to light-driven technologies (i.e., PG+) will require us to rethink wastewater treatment systems and ideally align resource (e.g., water, nutrients) consumption and recovery to the diurnal cycle of the sun. Constraining use and discharge of (waste-)water predominantly to the light periods of the day could be an effective tool to increase resource use efficiency and reduce our ecological footprint. This might be necessary to accommodate the needs of an ever-growing population and ensure a sustainable future.

5. Conclusion

In this study, we successfully integrated PAOs (i.e., Candidatus *Accumulibacter, Tetrasphaera* sp.) from AGS into native PGs and created a hybrid granule named PG+ performing photoEBPR. Thereby, PG+ significantly improved phosphorus recovery by 3–6x compared to native PG used in this study, photogranules from other studies and other microalgae-based technologies. Photoautotrophs, such as cyanobacteria and green algae, additionally generated metabolic energy from light and led to 2–3x higher biomass productivity of PG+ compared to AGS. Operating the PG+ system under a diurnal cycle of 12 h (light) and 12 h (dark) resulted in an 12-h anaerobic phase, which had no adverse effect on polyphosphate cycling or phototrophic activity. However, the short anaerobic phases during the 12 h daytime resulted in an overall lower light availability due to shorter aerobic phases and consequently reduced phototrophic growth. This decreased biomass productivity and nitrogen removal during operation under a natural diurnal cycle by around 30%. Therefore, we suggest reconsidering the bioreactor operation in sequencing batch mode and developing a continuous operation mode with separate anaerobic (dark) and aerobic (light) compartments. This would allow photogranules to maximally utilize the light input during daytime and optimize such a light-driven wastewater treatment system for operation under a natural diel cycle.

CRediT authorship contribution statement

Lukas M. Trebuch: Conceptualization, Methodology, Investigation, Visualization, Formal analysis, Writing – original draft. **Jasper Sohier:** Conceptualization, Methodology, Investigation, Formal analysis. **Sido Altenburg:** Conceptualization, Methodology. **Ben O. Oyserman:** Conceptualization, Methodology. **Mario Pronk:** Methodology, Writing – review & editing. **Marcel Janssen:** Supervision, Conceptualization, Writing – review & editing. **Louise E.M. Vet:** Supervision, Funding acquisition, Writing – review & editing. **René H. Wijffels:** Supervision, Writing – review & editing. **Tânia V. Fernandes:** Supervision, Conceptualization, Funding acquisition, Writing – review & editing.

Declaration of Competing Interest

The authors declare that they have no known competing financial interests or personal relationships that could have appeared to influence the work reported in this paper.

Data availability

Data will be made available on request.

Acknowledgements

The authors would like to thank Winifred Noorlander, who kindly provided the AGS inoculum, Nico Helmsing, for his excellent support with bioreactor operation and chemical analysis, and Ciska Raaijmakers, for chemical analysis. This research was supported by Stichting voor de Technische Wetenschappen (STW) under the grant number STW-15424.

Supplementary materials

Supplementary material associated with this article can be found, in the online version, at doi:10.1016/j.watres.2023.119748.

References

Abouhend, A.S., McNair, A., Kuo-Dahab, W.C., Watt, C., Butler, C.S., Milferstedt, K., Hamelin, J., Seo, J., Gikonyo, G.J., El-Moselhy, K.M., Park, C., 2018. The oxygenic photogranule process for aeration-free wastewater treatment. Environ. Sci. Technol. 52, 3503–3511. https://doi.org/10.1021/acs.est.8b00403.

Albertsen, M., Karst, S.M., Ziegler, A.S., Kirkegaard, R.H., Nielsen, P.H., 2015. Back to basics – The influence of DNA extraction and primer choice on phylogenetic analysis of activated sludge communities. PLoS ONE 10, e0132783. https://doi.org/10.1371/journal.pone.0132783.

APHA, AWWA, WEF, 2012. Standard Methods for the Examination of Water and Wastewater, 22nd ed. American Public Health Association, American Water Works Association, Water Environment Federation, Washington, DC.

Blanken, W., Cuaresma, M., Wijffels, R.H., Janssen, M., 2013. Cultivation of microalgae on artificial light comes at a cost. Algal. Res. 2, 333–340. https://doi.org/10.1016/j.algal.2013.09.004.

Borowitzka, M.A., 2013. High-value products from microalgae—Their development and commercialisation. J. Appl. Phycol. 25, 743–756. https://doi.org/10.1007/s10811-013-9983-9.

Brehm, U., Krumbein, W.E., Palińska, K.A., 2003. Microbial spheres: a novel cyanobacterial–diatom symbiosis. Naturwissenschaften 90, 136–140. https://doi.org/10.1007/s00114-003-0403-x.

Brockmann, D., Gérand, Y., Park, C., Milferstedt, K., Hélias, A., Hamelin, J., 2021. Wastewater treatment using oxygenic photogranule-based process has lower environmental impact than conventional activated sludge process. Bioresour. Technol. 319 https://doi.org/10.1016/j.biortech.2020.124204.

Cai, W., Zhao, Z., Li, D., Lei, Z., Zhang, Z., Lee, D.-J., 2019. Algae granulation for nutrients uptake and algae harvesting during wastewater treatment. Chemosphere 214, 55–59. https://doi.org/10.1016/j.chemosphere.2018.09.107.

Carvalho, V.C.F., Freitas, E.B., Silva, P.J., Fradinho, J.C., Reis, M.A.M., Oehmen, A., 2018. The impact of operational strategies on the performance of a photo-EBPR system. Water Res. 129, 190–198. https://doi.org/10.1016/j.watres.2017.11.010.

Carvalho, V.C.F., Kessler, M., Fradinho, J.C., Oehmen, A., Reis, M.A.M., 2021. Achieving nitrogen and phosphorus removal at low C/N ratios without aeration through a novel phototrophic process. Sci. Total Environ. 793, 148501 https://doi.org/10.1016/j.scitotenv.2021.148501.

Chen, G., Ekama, G.A., van Loosdrecht, M.C.M., Brdjanovic, D., 2020. Biological Wastewater Treatment: Principles, Modeling and Design. IWA Publishing. https://doi.org/10.2166/9781789060362.

Cieślik, B.M., Namieśnik, J., Konieczka, P., 2015. Review of sewage sludge management: standards, regulations and analytical methods. J. Clean. Prod. 90, 1–15. https://doi.org/10.1016/j.jclepro.2014.11.031.

Cuaresma Franco, M., Buffing, M.F., Janssen, M., Vílchez Lobato, C., Wijffels, R.H., 2012. Performance of Chlorella sorokiniana under simulated extreme winter conditions. J. Appl. Phycol. 24, 693–699. https://doi.org/10.1007/s10811-011-9687-y.

de Graaff, D.R., van Loosdrecht, M.C.M., Pronk, M., 2020. Biological phosphorus removal in seawater-adapted aerobic granular sludge. Water Res. 172, 115531 https://doi.org/10.1016/j.watres.2020.115531.

de Kreuk, M.K., Heijnen, J.J., van Loosdrecht, M.C.M., 2005. Simultaneous COD, nitrogen, and phosphate removal by aerobic granular sludge. Biotechnol. Bioeng. 90, 761–769. https://doi.org/10.1002/bit.20470.

de Kreuk, M.K., van Loosdrecht, M.C.M., 2004. Selection of slow growing organisms as a means for improving aerobic granular sludge stability. Water Sci. Technol. 49, 9–17. https://doi.org/10.2166/wst.2004.0792.

Flemming, H.C., Wingender, J., 2010. The biofilm matrix. Nat. Rev. Microbiol. 8, 623–633. https://doi.org/10.1038/nrmicro2415.

Gikonyo, J.G., Ansari, A.A., Abouhend, A.S., Tobiason, J.E., Park, C., 2021. Hydrodynamic granulation of oxygenic photogranules. Environ. Sci. Water Res. Technol. 7, 427–440. https://doi.org/10.1039/D0EW00957A.

Huang, W., Li, B., Zhang, C., Zhang, Z., Lei, Z., Lu, B., Zhou, B., 2015. Effect of algae growth on aerobic granulation and nutrients removal from synthetic wastewater by using sequencing batch reactors. Bioresour. Technol. 179, 187–192. https://doi.org/10.1016/j.biortech.2014.12.024.

Ji, B., Zhang, M., Wang, L., Wang, S., Liu, Y., 2020. Removal mechanisms of phosphorus in non-aerated microalgal-bacterial granular sludge process. Bioresour. Technol. 312, 123531 https://doi.org/10.1016/j.biortech.2020.123531.

Kehrein, P., Van Loosdrecht, M., Osseweijer, P., Garfí, M., Dewulf, J., Posada, J., 2020. A critical review of resource recovery from municipal wastewater treatment plants-market supply potentials, technologies and bottlenecks. Environ. Sci. Water Res. Technol. 6, 877–910. https://doi.org/10.1039/c9ew00905a.

Kleikamp, H.B.C., Pronk, M., Tugui, C., Guedes da Silva, L., Abbas, B., Lin, Y.M., van Loosdrecht, M.C.M., Pabst, M., 2021. Database-independent de novo metaproteomics of complex microbial communities. Cell Syst. 12, 375–383. https://doi.org/10.1016/j.cels.2021.04.003 e5.

Li, D., Yang, J., Li, Y., Zhang, J., 2021. Research on rapid cultivation of aerobic granular sludge (AGS) with different feast-famine strategies in continuous flow reactor and achieving high-level denitrification via utilization of soluble microbial product (SMP). Sci. Total Environ. 786, 147237 https://doi.org/10.1016/j.scitotenv.2021.147237.

Loosdrecht, M.C., Picioreanu, C., Heijnen, J.J., 1997. A more unifying hypothesis for biofilm structures. FEMS Microbiol. Ecol. 24, 181–183. https://doi.org/10.1111/j.1574-6941.1997.tb00434.x.

Lopez-Vazquez, C.M., Oehmen, A., Hooijmans, C.M., Brdjanovic, D., Gijzen, H.J., Yuan, Z., van Loosdrecht, M.C.M., 2009. Modeling the PAO-GAO competition: effects of carbon source, pH and temperature. Water Res. 43, 450–462. https://doi.org/10.1016/j.watres.2008.10.032.

Louca, S., Parfrey, L.W., Doebeli, M., 2016. Decoupling function and taxonomy in the global ocean microbiome. Science (80-.) 353, 1272–1277. https://doi.org/10.1126/science.aaf4507.

Louca, S., Polz, M.F., Mazel, F., Albright, M.B.N., Huber, J.A., O'Connor, M.I., Ackermann, M., Hahn, A.S., Srivastava, D.S., Crowe, S.A., Doebeli, M., Parfrey, L.W., 2018. Function and functional redundancy in microbial systems. Nat. Ecol. Evol. 2, 936–943. https://doi.org/10.1038/s41559-018-0519-1.

Meng, F., Xi, L., Liu, D., Huang, W.W., Lei, Z., Zhang, Z., Huang, W.W., 2019. Effects of light intensity on oxygen distribution, lipid production and biological community of algal-bacterial granules in photo-sequencing batch reactors. Bioresour. Technol. 272, 473–481. https://doi.org/10.1016/j.biortech.2018.10.059.

Milferstedt, K., Kuo-Dahab, W.C., Butler, C.S., Hamelin, J., Abouhend, A.S., Stauch-White, K., McNair, A., Watt, C., Carbajal-González, B.I., Dolan, S., Park, C., 2017. The importance of filamentous cyanobacteria in the development of oxygenic photogranules. Sci. Rep. 7, 17944. https://doi.org/10.1038/s41598-017-16614-9.

Mohamed, A.Y.A., Welles, L., Siggins, A., Healy, M.G., Brdjanovic, D., Rada-Ariza, A.M., Lopez-Vazquez, C.M., 2021. Effects of substrate stress and light intensity on enhanced biological phosphorus removal in a photo-activated sludge system. Water Res. 189, 116606 https://doi.org/10.1016/j.watres.2020.116606.

Nancharaiah, Y.V., Kiran Kumar Reddy, G., 2018. Aerobic granular sludge technology: mechanisms of granulation and biotechnological applications. Bioresour. Technol. 247, 1128–1143. https://doi.org/10.1016/j.biortech.2017.09.131.

Nierychlo, M., Andersen, K.S., Xu, Y., Green, N., Jiang, C., Albertsen, M., Dueholm, M.S., Nielsen, P.H., 2020. MiDAS 3: an ecosystem-specific reference database, taxonomy and knowledge platform for activated sludge and anaerobic digesters reveals species-level microbiome composition of activated sludge. Water Res. 182, 115955 https://doi.org/10.1016/j.watres.2020.115955.

Oyserman, B.O., Martirano, J.M., Wipperfurth, S., Owen, B.R., Noguera, D.R., McMahon, K.D., 2017. Community assembly and ecology of activated sludge under photosynthetic feast–famine conditions. Environ. Sci. Technol. 51, 3165–3175. https://doi.org/10.1021/acs.est.6b03976.

Pijuan, M., Ye, L., Yuan, Z., 2010. Free nitrous acid inhibition on the aerobic metabolism of poly-phosphate accumulating organisms. Water Res. 44, 6063–6072. https://doi.org/10.1016/j.watres.2010.07.075.

Pronk, M., de Kreuk, M.K., de Bruin, B., Kamminga, P., Kleerebezem, R., van Loosdrecht, M.C.M., 2015. Full scale performance of the aerobic granular sludge process for sewage treatment. Water Res. 84, 207–217. https://doi.org/10.1016/j.watres.2015.07.011.

Risgaard-Petersen, N., Nicolaisen, M.H., Revsbech, N.P., Lomstein, B.A., 2004. Competition between ammonia-oxidizing bacteria and benthic microalgae. Appl. Environ. Microbiol. 70, 5528–5537. https://doi.org/10.1128/AEM.70.9.5528-5537.2004.

Slegers, P.M., Lösing, M.B., Wijffels, R.H., van Straten, G., van Boxtel, A.J.B., 2013. Scenario evaluation of open pond microalgae production. Algal. Res. 2, 358–368. https://doi.org/10.1016/j.algal.2013.05.001.

Stokholm-Bjerregaard, M., McIlroy, S.J., Nierychlo, M., Karst, S.M., Albertsen, M., Nielsen, P.H., 2017. A critical assessment of the microorganisms proposed to be important to enhanced biological phosphorus removal in full-scale wastewater treatment systems. Front. Microbiol. 8, 1–18. https://doi.org/10.3389/fmicb.2017.00718.

Suleiman, A.K.A., Lourenço, K.S., Clark, C., Luz, R.L., da Silva, G.H.R., Vet, L.E.M., Cantarella, H., Fernandes, T.V., Kuramae, E.E., 2020. From toilet to agriculture: fertilization with microalgal biomass from wastewater impacts the soil and rhizosphere active microbiomes, greenhouse gas emissions and plant growth. Resour. Conserv. Recycl. 161, 104924 https://doi.org/10.1016/j.resconrec.2020.104924.

Sun, Y., Angelotti, B., Wang, Z.W., 2019. Continuous-flow aerobic granulation in plug-flow bioreactors fed with real domestic wastewater. Sci. Total Environ. 688, 762–770. https://doi.org/10.1016/j.scitotenv.2019.06.291.

Takeuchi, N., Kohshima, S., Seko, K., 2001. Structure, formation, and darkening process of albedo-reducing material (cryoconite) on a himalayan glacier: a granular algal mat growing on the glacier. Arctic, Antarct. Alp. Res. 33, 115. https://doi.org/10.2307/1552211.

Tiron, O., Bumbac, C., Patroescu, I.V., Badescu, V.R., Postolache, C., 2015. Granular activated algae for wastewater treatment. Water Sci. Technol. 71, 832–839. https://doi.org/10.2166/wst.2015.010.

Trebuch, L.M., 2022. Photogranules For Wastewater Treatment : From Community Assembly to Targeted Microbial Functions. Wageningen University. https://doi.org/10.18174/562026.

Trebuch, L.M., Oyserman, B.O., Janssen, M., Wijffels, R.H., Vet, L.E.M., Fernandes, T.V., 2020. Impact of hydraulic retention time on community assembly and function of photogranules for wastewater treatment. Water Res. 173, 115506 https://doi.org/10.1016/j.watres.2020.115506.

Vishniac, W., Santer, M., 1957. The *thiobacilli*. Bacteriol. Rev. 21, 195–213.

Wang, M., Yang, H., Ergas, S.J., van der Steen, P., 2015. A novel shortcut nitrogen removal process using an algal-bacterial consortium in a photo-sequencing batch reactor (PSBR). Water Res. 87, 38–48. https://doi.org/10.1016/j.watres.2015.09.016.

Wang, X., Wen, X., Yan, H., Ding, K., Zhao, F., Hu, M., 2011. Bacterial community dynamics in a functionally stable pilot-scale wastewater treatment plant. Bioresour. Technol. 102, 2352–2357. https://doi.org/10.1016/j.biortech.2010.10.095.

Weissbrodt, D.G., Neu, T.R., Kuhlicke, U., Rappaz, Y., Holliger, C., 2013. Assessment of bacterial and structural dynamics in aerobic granular biofilms. Front. Microbiol. 4, 1–18. https://doi.org/10.3389/fmicb.2013.00175.